

Tetragonal-Orthorhombic Structural Modulation at Low Temperature in $\text{La}_{2-x}\text{Ba}_x\text{CuO}_4$

Yimei Zhu, A. R. Moodenbaugh, Z. X. Cai, J. Tafto,* M. Suenaga, and D. O. Welch

Materials Science Division, Brookhaven National Laboratory, Upton, New York 11973

(Received 21 June 1994)

Below ~ 60 K $\text{La}_{2-x}\text{Ba}_x\text{CuO}_4$ ($0.10 \leq x \leq 0.15$) reveals superstructure reflections consistent with the tetragonal space group $P4_2/ncm$ [low temperature tetragonal (LTT)]. However, twins, characteristic of the related orthorhombic phase [low temperature orthorhombic (LTO)], persist in this material. Electron microscopy shows that the LTT superstructure reflections originate from the twin-boundary region. This suggests a phase mixture of orthorhombic and tetragonal with a gradual change from LTO (space group $Bmab$) in the interior of the twin domains, via the $Pccn$, to LTT at the twin boundary. This is modeled as a spatial modulation, the tipping angle of CuO_6 octahedra being an order parameter.

PACS numbers: 74.72.Dn, 61.72.Mm

The phase diagram of $\text{La}_{2-x}\text{Ba}_x\text{CuO}_4$ and its relationship to the superconducting transition temperature T_c is intriguing. In the closely related system $\text{La}_{2-x}\text{Sr}_x\text{CuO}_4$, T_c for Sr content $x \geq 0.05$ rises nearly monotonically until it reaches its broad maximum of about 30 K at $x = 0.15$, then monotonically drops to zero at $x \approx 0.32$ [1]. The general trend is similar for $\text{La}_{2-x}\text{Ba}_x\text{CuO}_4$ except for the important difference that a drastic reduction in T_c is observed for $0.10 < x < 0.15$ with a local minimum below 4 K at $x \approx 0.125$ [2]. In the concentration range of the local T_c minimum in $\text{La}_{2-x}\text{Ba}_x\text{CuO}_4$ there is evidence of a low temperature tetragonal (LTT) structure with proposed space group $P4_2/ncm$ below about 60 K [2,3]. Above this temperature the structure is orthorhombic (LTO) with space group $Bmab$ and, for higher temperatures, again tetragonal (HTT) with the space group $I4/mmm$. For consistency we will index diffraction spots in HTT using the LTO unit cell ($a \approx b \approx 5.37$ Å, $c \approx 11.2$ Å). Table I serves as a guide to those readers not familiar with the extinction rules of the phases involved in this Letter. There the allowed reflections of the HTT phase are referred to as the fundamental reflections.

The transition from HTT to LTO during cooling results in twins [4,5]. The normal to the twin boundaries is the [110] direction or the equivalent $[-110]$ direction ($Bmab$ setting). For a Ba content of $x = 0.12$, the structure is HTT at room temperature and transforms to orthorhombic at about 200 K. Below 60 K, neutron diffraction studies show that there is a phase transition from LTO to LTT [2]. It has been reported that there was little change in twin morphology, even when the sample was cooled down to 10 K in a transmission electron microscope (TEM) [4]. This is inconsistent with pure LTT phase, since the twinning is associated with an orthorhombic symmetry. To address the issue of the LTO/LTT phase transition, we performed *in situ* experiments with a 200 keV TEM equipped with a low temperature (liquid He) specimen holder. Samples are prepared by a procedure previously described [6]. The TEM specimens were thinned by ion milling with a low-energy gun.

Figure 1 shows the temperature dependence of the microstructure and the corresponding diffraction pattern of a $\text{La}_{1.88}\text{Ba}_{0.12}\text{CuO}_4$ specimen observed *in situ*, while being heated from 20 to 250 K. At about 20 K, fine twins are the predominant microstructural feature of the crystal [Fig. 1(a)]. With increasing temperature, first some needlelike twins disappear [Fig. 1(d), ~ 140 K] with the specimen being twin-free above 200 K [Fig. 1(g), ~ 250 K], where the sample becomes HTT. It should be noted that the twin morphology is not always reversible after a thermal cycle. We often observed an increased density of fine twins at low temperature after cycling.

The structural transitions can be elucidated by analyzing the electron diffraction. Shown also in Fig. 1 are the corresponding diffraction patterns of the $(001)^*$ [Figs. 1(b), 1(e), and 1(h)] and $(101)^*$ [Figs. 1(c), 1(f), and 1(i)] zone axes at 20, 140, and 250 K, respectively. At 250 K, Figs. 1(h) and 1(i) clearly indicate the $I4/mmm$ space group (HTT phase), because only the fundamental reflections are present.

In contrast, at about 140 K, superstructure reflections in accordance with the LTO phase (Table I) appear in $(101)^*$ projection. Below about 60 K, in $(001)^*$ projection, additional superstructure spots are visible for $h + k = 2n$ with h and k odd, e.g., the (110), (130) reflection, etc. The presence of (110) type reflections, which are forbidden in LTO phase, is allowed for the space group $P4_2/ncm$ predicted for the LTT phase, and also for the space group $Pccn$ [low temperature less orthorhombic (LTLO) phase], that was proposed to account for the presence of a considerable orthorhombic strain [7]. However, the $(101)^*$ diffraction pattern remains the same, because $h + l = 2n$ reflections are allowed in all of the $Bmab$, $P4_2/ncm$, and $Pccn$ space groups.

Compared to neutron and x-ray diffractions, one advantage of electron diffraction is the sensitivity to weak intensities. However, a disadvantage is that it also can produce double diffraction, when a reflected electron beam acts as a new incident beam. In $(001)^*$ projection [Fig. 1(b)] at low temperature we also observe weak superstructure spots

TABLE I. A summary of the crystallography of $\text{La}_{1.88}\text{Ba}_{0.12}\text{CuO}_4$ and the expected superstructure reflections in the $(101)^*$, $(011)^*$, and $(001)^*$ projections. HTT and LTT are high- and low-temperature tetragonal, respectively; LTO and LTLO are low-temperature orthorhombic and less orthorhombic, respectively.

Temperature	Phase	Space group	Allowed superstructure reflections for projection		
			$(101)^*$	$(011)^*$	$(001)^*$
$T > 200$ K	HTT	$I4/mmm^a$	none	none	none
$200 > T > 60$ K	LTO	$Bmab^b$	$h + l = 2n$	none	none
$T < 60$ K	LTLO	$Pccn^c$	$h + l = 2n$	none	$h + k = 2n, h, k = \text{odd}$
	LTT	$P4_2/ncm^c$	$h + l = 2n$	none	$h + k = 2n, h, k = \text{odd}$

^aWe use indexing for the expanded $\sqrt{2}$ cell for HTT.

^b $Cmca$ is the standard setting for LTO, we use $Bmab$ for indexing consistency.

^cExtinction rules are identical for LTLO and LTT.

at (100) , (010) , (210) , etc. Some may be too weak to be reproduced here. According to the extinction rule of both space group $P4_2/ncm$ and $Pccn$, the reflections at $h + k = 2n + 1$ should be absent. We attribute these spots to the double scattering involving large \mathbf{g} vectors in the first or higher order Laue zones where $l = 1, 3, \dots, 2n + 1$. The intensity of the (100) type spots increases with a decrease of temperature, as is to be expected, because of the increased coupling via large \mathbf{g} vectors when the Debye-Waller factor is reduced.

Double scattering to the (110) -type reciprocal-lattice coordinates is, in principle, possible if twins stacked up

along the incident electron beam are rotated 90° . However, the observation that the (110) -type reflections are much stronger than (100) -type reflection appears to rule out the possibility that double scattering is the major contributor to the (110) -type reflections in accordance with a previous electron diffraction [5]. Further evidence that the (110) -type reflections are real is that they appear in the electron diffraction patterns at about the temperature where the transition from LTO to LTT takes place according to neutron diffraction studies [2–4].

It is possible to use the distinctive superstructure reflections associated with LTO and LTT phases to image the location of the corresponding phases. A previous attempt to accomplish this was unsuccessful, possibly due to insufficient intensity and contrast [4]. With a specially designed objective aperture ($5 \mu\text{m}$ in diameter), we were able to record dark-field images using these weak superstructure reflections.

Figure 2 shows three enlarged micrographs from the rectangular area shown in Fig. 1(a), for a nominal temperature of 20 K. Figure 2(a) is imaged 22° away from the c axis of the same area in alternatively the $[101]$ and the twin related $[011]$ orientation. Since the (121) superstructure spot in the $(101)^*$ projection [marked by a circle pin Fig. 1(c)] was used to form the image, only every second twin [(101) oriented] is bright, as is evident from the extinction rules, see Table I. Figure 2(b) is a bright-field image showing the area morphology with twin boundaries edge on in the (001) orientation. An intriguing observation in this orientation is the narrow bright lines in the dark field image of Fig. 2(c), using the LTT-phase-related (110) reflection in the $(001)^*$ projection [marked by a circle in Fig. 1(b)]. By comparison with Fig. 2(b) these narrow lines occur at the twin boundary, suggesting that the LTT phase is located at the regions of twin boundaries [the arrow marked in Figs. 2(a), 2(b), and 2(c) indicates the same twin domain]. Similar images were also obtained at a nominal temperature of about 50 K (the overall specimen temperature, although we do not know the exact local

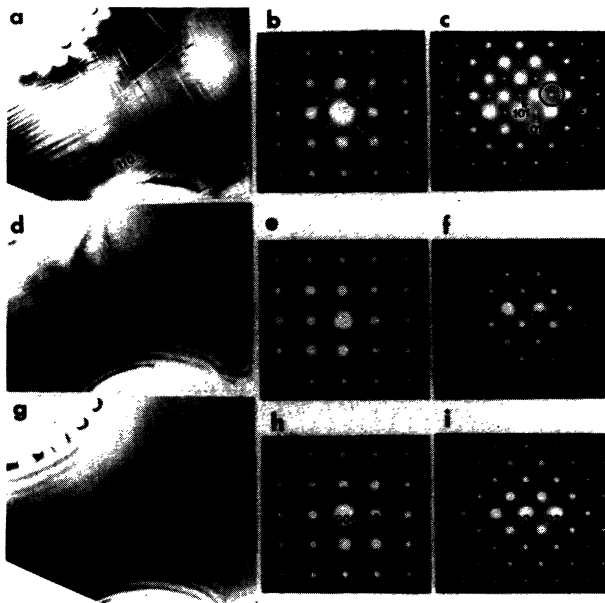


Fig. 1. Temperature dependence of microstructure and diffraction patterns of $\text{La}_{1.88}\text{Ba}_{0.12}\text{CuO}_4$ at 20 K [(a)–(c)], 140 K [(d)–(f)], and 250 K [(g)–(i)]. (b), (e), and (h) are diffraction patterns of the $(001)^*$ zone, while (c), (f), and (i) are of the $(101)^*$ zone. Note the diffraction of the $(001)^*$ projection of HTT phase (h) and LTO phase (e) are identical, and the $(101)^*$ projection of the LTO (f) and LTT phase (c) are identical.

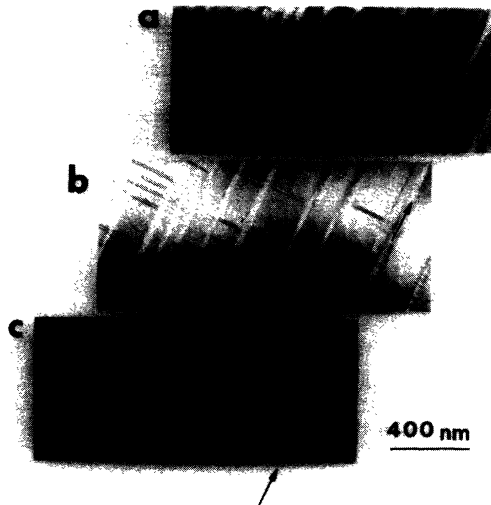


FIG. 2. Diffraction contrast observed at 20 K from the area bounded by a rectangular box shown in Fig. 1(a). (a) The dark-field image using the LTO superlattice reflection (121) of the (101)* projection [see Fig. 1(c)]. Note that the twin boundaries are inclined and only one set of the twin domains shows contrast. (b) The bright-field image in the [001] orientation. The twin boundaries are edge on. (c) The dark-field image viewed in the same orientation as (b) but using the LTT superlattice reflection (110) [see Fig. 1(b)]. Note that only the twin boundaries show the bright contrast suggesting that they are the corresponding LTT phase.

temperature due to the electron beam heating) for a specimen with Ba content of $0.09 < x < 0.12$ but are not seen for pure La_2CuO_4 at room temperature. The intensity profile and thickness of the layer at the twin boundary are hard to estimate due to the intrinsic low intensity of the superstructure reflections. The thickness of the LTT phase is probably of the order of 100 Å, which is very close to the value predicted (a few hundred Å) from an observation of the broadening of the superlattice peaks of the LTT phase by neutron diffraction.

The presence of the LTT phase at the location of the LTO twin boundary is consistent with the crystallography of the tipping of the CuO_6 octahedra. In the LTO phase, the CuO_6 octahedra are tilted a few degrees around the [100] axis. The results in a conflict at the twin boundary such that the two twin domains have displacements in orthogonal directions, as indicated in Fig. 3(a). Thus, from simple geometrical considerations an ideally sharp twin boundary, which is likely to have a very high interfacial energy (especially near the LTO/LTT transition temperature, due to the increased orthorhombicity of the LTO phase), is incompatible with the required tilting of the octahedron. Possible configurations are either a localized twin boundary with severely distorted octahedra at the boundary or extended twin-boundary regions where the structure gradually changes from orthorhombic to tetragonal. We propose a delocalized boundary with LTT structure at the center of the twin boundary, gradually changing via the or-

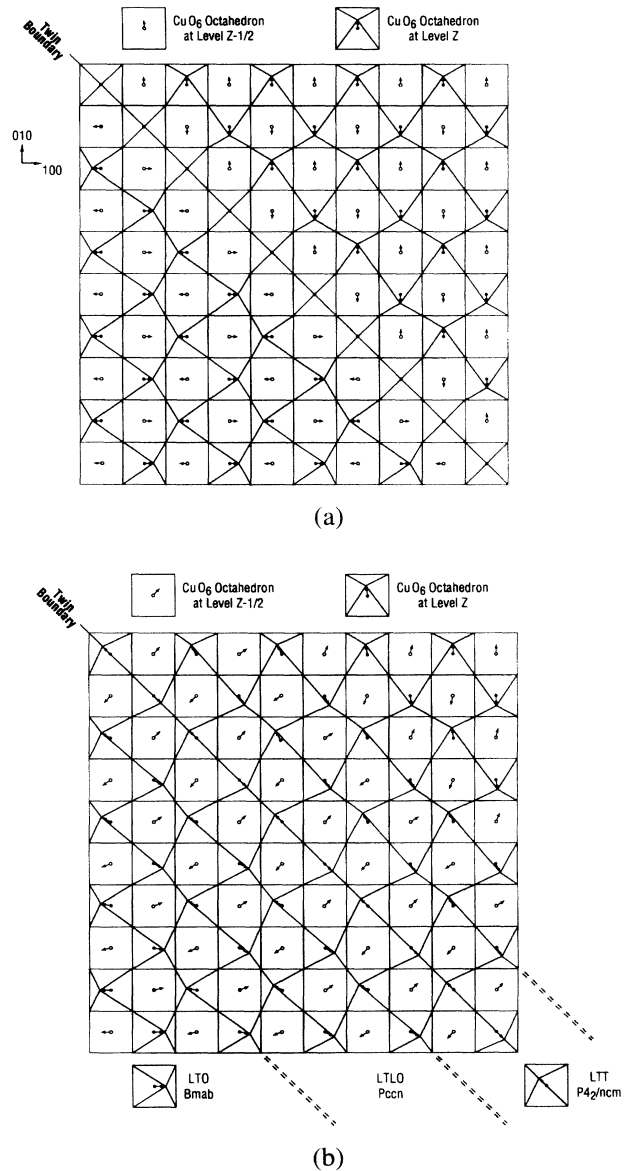


FIG. 3. (a) An ideal twin boundary in the LTO structure results in a conflict between the tilting of the CuO_6 octahedra around the [100] and [010] axes. The resultant is tilting around the [110] axis. (b) The proposed model in which the LTT structure (tipping axis [110]) exists at the center of the twin boundaries with a gradual transition, via the LTLO structure, to LTO (tipping axis [100]) in the center of the twin domain.

thorhombic *Pccn* (LTLO) to an orthorhombic LTO in the center of the twin matrix as shown in Fig. 3(b). The LTT phase appears to nucleate at and grow out from the LTO twin boundaries, where the conflict of the tipping axis between the adjacent twins is resolved. Further cooling of the specimens of $\text{La}_{2-x}\text{Ba}_x\text{CuO}_4$ ($0.09 < x < 0.12$) through the LTO phase results in an increasing twin density, and thus a larger volume of the LTT phase. The observed hysteresis in developing the low temperature twins during

our *in situ* thermal cycling implies that kinetics plays an important role in formation of the LTT phase. Figure 3(b) also suggests that the orthorhombic $Pccn$ is located at the LTT/LTO interphase region and acts as a buffer structure. This is consistent with previous neutron studies [7,8] which predict the existence of the LTLO phase and a continuous phase transition of LTO-LTLO-LTT in a finite temperature region. The present results appear to contradict the recent findings of Billinge *et al.* of a predominantly tetragonal phase [9]; however, we note that the analysis on which that conclusion was based assumes a *discrete* orthorhombic phase, not the phase with varying orthorhombicity that has been observed in the TEM studies here and previously [5]. A twin boundary with a structure different from twin matrix has been observed at room temperature in $PbVO_4$, using high resolution electron microscopy [10].

To further study the structure, the width, and the density of twin boundaries in LTO phase using a theoretical approach, we considered the possibility that the twin boundary could be LTT or HTT. We compared the free energy of twin boundaries with LTT to those with HTT structure using a Landau-type free energy model. The details will be published elsewhere [11]. The model utilizes the order parameter expansion of Ishibashi [12], which reproduces the composition-temperature phase diagram of $La_{2-x}Ba_xCuO_4$. The numerical calculations showed that LTT boundary, as shown in Fig. 3(b), is favored at low temperature, and LTT becomes the predominant structure if annealing time is long enough. However, because of the low LTO-LTT transition temperature (≈ 60 K), the growth of the LTT domain may be very slow. The morphology of the system will then consist of quasiperiodic domains of the LTO-LTT-LTO modulated structure, as shown in Fig. 2. An anharmonic lattice dynamical model for $La_{2-x}Ba_xCuO_4$ with parameters obtained from the first principle calculations [13] predicts that the LTO to LTT transition is a vibrational-entropy-driven first-order phase transition [11]. A quenched sample can thus retain metastable LTO domains with the LTT twin boundaries serving as nuclei for the growth of LTT phase. The structure modulation is also consistent with the small energy differences (≈ 15 meV per CuO_6 octahedron [13]) between LTO and LTT phase.

In summary, electron microscopy provides evidence that, at low temperature, $La_{1.88}Ba_{0.12}CuO_4$ consists of

a mixture of orthorhombic and tetragonal phases, the latter located in the twin boundary regions. The model proposed here features a gradual change from LTT at the twin boundary sites to LTO in the twin matrix.

This work was supported by the Division of Materials Sciences, U.S. Department of Energy under Contract No. DE-AC02-76CH00016.

*Visiting scientist from University of Oslo, Department of Physics, Blindern, Norway.

- [1] J. B. Torrance, Y. Tokura, A. I. Nazzari, A. Beziere, T. C. Huang, and S. S. P. Parkin, *Phys. Rev. Lett.* **61**, 1127 (1988).
- [2] J. D. Axe, A. H. Moudden, D. Hohlwein, D. E. Cox, K. M. Mohanty, A. R. Moodenbaugh, and Y. Xu, *Phys. Rev. Lett.* **62**, 2751 (1989).
- [3] J. D. Axe, D. E. Cox, K. Mohanty, H. Moudden, A. R. Moodenbaugh, Y. Xu, and T. R. Thurston, *IBM J. Res. Dev.* **33**, 382 (1989).
- [4] C. H. Chen, S. W. Cheong, D. J. Werder, A. S. Copper, and L. W. Rupp, Jr., *Physica (Amsterdam)* **175C**, 301 (1991).
- [5] C. H. Chen, S. W. Cheong, D. J. Werder, and H. Takagi, *Physica (Amsterdam)* **206C**, 183 (1993).
- [6] A. R. Moodenbaugh, Y. Xu, M. Suenaga, T. J. Folkerts, and R. N. Shelton, *Phys. Rev. B* **38**, 4596 (1988).
- [7] D. E. Cox, P. Zolliker, J. D. Axe, A. H. Moudden, A. R. Moodenbaugh, and Y. Xu, *Mater. Res. Soc. Symp. Proc.* **156**, 141 (1989).
- [8] J. D. Axe, in *Proceedings of the Conference on Lattice Effects in High- T_c Superconductors, Santa Fe, New Mexico, 1992*, edited by Y. Bar-Yam, T. Egami, J. Mustre-de Leon, and A. R. Bishop (World Scientific, Singapore, 1992), pp. 517–530.
- [9] S. J. L. Billinge, G. H. Kwei, A. C. Lawson, J. D. Thompson, and H. Takagi, *Phys. Rev. Lett.* **71**, 1903 (1993).
- [10] C. Manolikas, G. Van Tendeloo, and S. Amelinckx, *Solid State Commun.* **58**, 851 (1986).
- [11] Z. X. Cai and D. O. Welch, *Physica (Amsterdam)* **231C**, 383 (1994).
- [12] Y. Ishibashi, *J. Phys. Soc. Jpn.* **59**, 800 (1990); Y. Ishibashi and I. Suzuki, *ibid.* **53**, 903 (1984).
- [13] W. E. Pickett, R. E. Cohen, and H. Krakauer, *Phys. Rev. Lett.* **67**, 228 (1991).

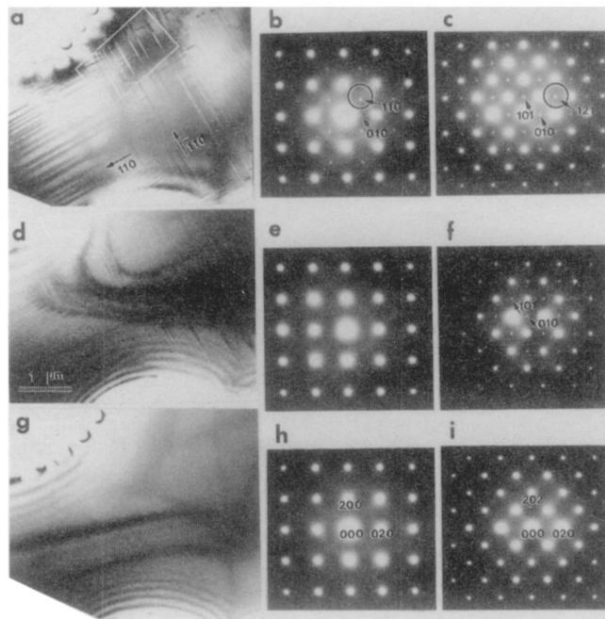


Fig. 1. Temperature dependence of microstructure and diffraction patterns of $\text{La}_{1.88}\text{Ba}_{0.12}\text{CuO}$ at 20 K [(a)–(c)], 140 K [(d)–(f)], and 250 K [(g)–(i)]. (b), (e), and (h) are diffraction patterns of the (001)* zone, while (c), (f), and (i) are of the (101)* zone. Note the diffraction of the (001)* projection of HTT phase (h) and LTO phase (e) are identical, and the (101)* projection of the LTO (f) and LTT phase (c) are identical.

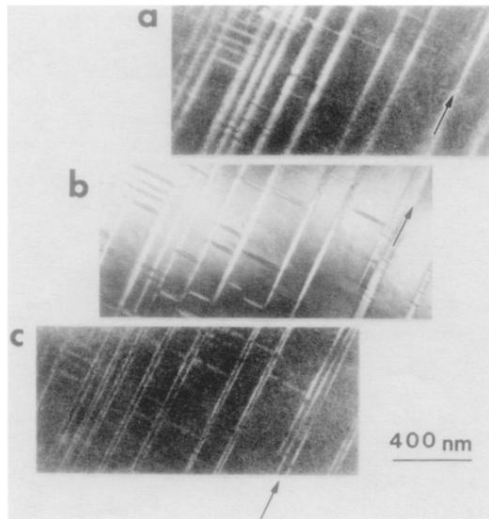


FIG. 2. Diffraction contrast observed at 20 K from the area bounded by a rectangular box shown in Fig. 1(a). (a) The dark-field image using the LTO superlattice reflection (121) of the (101)* projection [see Fig. 1(c)]. Note that the twin boundaries are inclined and only one set of the twin domains shows contrast. (b) The bright-field image in the [001] orientation. The twin boundaries are edge on. (c) The dark-field image viewed in the same orientation as (b) but using the LTT superlattice reflection (110) [see Fig. 1(b)]. Note that only the twin boundaries show the bright contrast suggesting that they are the corresponding LTT phase.